ACS ES&T Water

pubs.acs.org/estwater

Article

Different Fitness Costs during Biofilm Growth from Antibiotic-Resistant Bacteria to Antibiotic-Sensitive Bacteria under the Toxicity Stress of Copper Substrate

Min Chen,[§] Jiaping Wang,[§] Longji Xia, Guiying Li, Wanjun Wang, and Taicheng An*

Cite This: *ACS EST Water* 2025, 5, 1546−1556

Read Online

ACCESS | Metrics & More | Article Recommendations | Supporting Information

ABSTRACT: In water supply systems, copper pipes are commonly used to prevent bacterial growth and biofilm formation. However, it is uncertain whether copper can effectively inhibit antibiotic-resistant bacterial (ARB) biofilm formation, which is crucial for water supply safety. This study examined the difference in biofilm formation between ARB and antibiotic-sensitive bacteria (ASB) on copper surfaces by measuring the extracellular polymeric substance (EPS) content. In the blank control group, ASB biofilms outperformed ARB biofilms; however, when exposed to copper, the bacterial abundance of ARB biofilms was $10^{0.5}$−$10^{1.0}$ times higher than that of ASB biofilms, and the EPS content was also $10^{1.1}$−$10^{1.9}$ times higher. This disparity was mainly attributed to the varying fitness costs of the ARB in different environments. Furthermore, the oxidative stress response of ARB was significantly lower than that of ASB on a copper substrate, and the intracellular reactive oxygen species (ROS) level in ARB was only 78.7% of that of ASB. Gene expression patterns revealed that ARB biofilm formation on the copper substrate was mainly caused by the c-di-GMP-activated signaling pathway rather than the SOS stress system activated by ROS. These findings have implications for the choice of copper products in water supply systems.

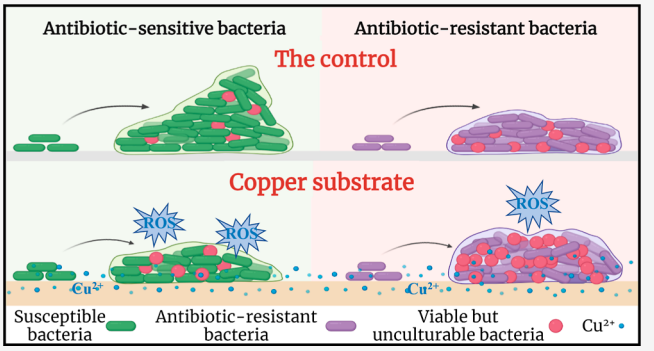

KEYWORDS: *antibiotic-resistant bacteria, antibiotic-sensitive bacteria, bacterial biofilm growth, copper substrate toxicity stress, c-di-GMP activated signaling*

1. INTRODUCTION

Legislation and policy in countries worldwide have showcased the challenges in achieving water security for improved quality of life.[1,2] Water supply safety concerns are becoming increasingly severe due to the emergence and spread of extensive antibiotic-resistant bacteria (ARB) and antibiotic resistance genes (ARGs).[3] Residual chlorine can persistently alter the composition of ARGs and increase the risk of ARB in water supply system.[4] Drinking water safety is significantly related to gastrointestinal diseases, including those caused by pathogenic *Escherichia coli* (*E. coli*).[5,6]

Various measures have been implemented to improve water quality.[7] Copper pipes and products are popular choices for water supply and heating systems due to their natural ability to kill bacteria by destroying cell membranes,[8] causing leakage of intracellular components that ultimately leads to cell death.[9,10] However, there has been an increasing number of reports concerning ARB,[11,12] bringing into question whether copper products can still inhibit their growth; because of this, the formation of ARB biofilms on copper products needs to be further investigated.

Previous research has indicated that copper substrates can inhibit the formation of biofilms by antibiotic-sensitive bacteria (ASB).[13] However, the impact of copper substrates on ARB biofilms has yet to be thoroughly investigated. This study aimed to examine the growth of the ARB biofilm and ASB biofilm on copper substrates from the perspective of antibiotic resistance mechanisms. Various factors, including the production of hydrolases, changes in antibiotic targets, cell membrane permeability, and the expression of efflux systems, may influence bacterial antibiotic resistance.[14] Most antibiotic resistance mechanisms are associated with adaptation costs, typically resulting in a reduced bacterial growth rate.[15,16] The magnitude of this cost is the main biological parameter that influences the development rate of antibiotic resistance and the stability of antibiotic resistance.[17] Plasmids play a significant role in bacterial ecology and evolution through horizontal gene transfer,[18] but carrying plasmids can burden bacterial

Received: June 29, 2024
Revised: November 27, 2024
Accepted: February 10, 2025
Published: February 21, 2025

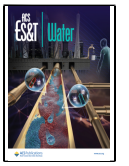

https://doi.org/10.1021/acsestwater.4c00603
ACS EST Water 2025, 5, 1546−1556

physiology and decrease adaptiveness;[17] the fitness cost associated with plasmids can also limit their persistence in bacterial populations.[19] Although the fitness cost of bacteria carrying ARG plasmids has been studied,[20,21] their impact on ARB biofilms in different environments is still unclear.

Two representative *E. coli* strains (ASB) *E. coli* DH5α and ARB *E. coli* DH5α (CTX) (carrying a cefotaxime (CTX) resistance plasmid) were used to culture biofilms on a copper substrate, with a blank substrate serving as a control. The resistance of the ARB biofilm and ASB biofilm to different antibiotics was characterized, and the intrinsic reasons behind the differences in antibiotic resistance between the two were assessed by examining efflux pump-related gene expression. Finally, the changes in oxidative stress in bacteria in biofilms were examined through evaluating the expression of oxidative stress- and biofilm growth-related genes. The study demonstrated varying fitness costs and intrinsic causes for the growth of the ARB biofilm and ASB biofilm under copper substrate stress, raising concerns regarding the use of copper pipes and products in water supply and heating systems.

2. MATERIALS AND METHODS

2.1. Construction of Target Strain and Culture Conditions. As *E. coli* is an enteric pathogenic bacterium that is significantly associated with gastrointestinal diseases related to drinking water distribution,[22,23] *E. coli* DH5α and *E. coli* DH5α (CTX) were used as representative strains of ASB and ARB, respectively. *E. coli* DH5α (CTX) was created by introducing the Incl-2 plasmid containing the $bla_{ctx\text{-}1}$ gene (resistance to CTX) by us as described in Text S1 and Figure S1. The specific construction operations (extraction of plasmid, transformation of competent cells, and introduction of plasmid) are presented in Texts S2−S4. These strains were cultured overnight in Luria−Bertani (LB) broth medium at 37 °C and then transferred to the biofilm culture device for biofilm cultivation.

2.2. Biofilm Formation and Culture Conditions. Each bacterial strain (200 μL, 10^9 colony-forming units (CFU)/mL) was inoculated in the multichannel biofilm culture device (Figure S2) with copper substrate as the biofilm attachment material. In real-world conditions, bacterial attachment is the first step of biofilm growth and is very time-consuming.[24] However, in this study, artificial attachment was used to accelerate the formation of biofilms. More details regarding the biofilm culture device are provided in Text S5. A 200 μL aliquot of the bacterial culture was absorbed and dropped along the upper edge of the device. The peristaltic pump was started after air drying and complete attachment of the culture to the copper surface in the bacterial liquid path for 2 h. The M9 low salt broth (Sangon Biotech) (to simulate the low nutrient environment in a real pipeline) was added into the culture tank at a flow rate of 1.2 mL/min to culture the biofilm. The concentration of active ingredients in M9 low salt broth with that in the real water supply systems was compared in Table S1. After a few days of culture, the biofilm grew along the solution trickle path. The image of the mature biofilm is shown in Figure S3.

Simultaneously, another group (only quartz glass as the attachment material) was also cultured to obtain biofilms of both strains. Biofilm samples were taken every 8 h until 96 h of culture for further characterization. Whenever a fixed sampling time was reached, the biofilms from one device were scraped off and resuspended in 5 mL of 0.01 M phosphate-buffered saline (PBS) for further analysis. Our previous findings indicate that biofilms reach maturity in 3−4 d, with the biomass peaking before entering the dispersion stage.[13,25] As this work mainly focused on the colonization disparities between ARB and ASB on the copper substrate, the biofilms were sampled in the first 4 days (96 h) for subsequent tests. Details about bacterial incubation and biofilm development are provided in Text S6. The surface morphology and composition of the copper substrate were characterized using X-ray diffraction (Rigaku Co., Japan), and diffraction peaks were perfectly directed to the materials (Figure S4). Each experiment was conducted independently in three repeats.

2.3. Visualization and Quantification of Biofilm Formation. Structures of biofilms sampled at different culture times were visualized by confocal laser scanning microscopy (CLSM). Briefly, 10 μL aliquot of biofilms from different channels in the biofilm culture device was placed on microscope slides. Samples were stained with SYTO 9 from the LIVE/DEAD Backlight kit (Thermo Fisher Scientific, USA), and 3D morphologies were observed under CLSM (LSM 800 with Airyscan, Carl Zeiss, Germany). Bacteria stained with SYTO 9 emit green light when excited by a 488 nm laser. Biofilm biomass was quantified using the plate count method.[13] The concentrations of protein and polysaccharide in extracellular polymeric substance (EPS) of biofilm were quantified with the improved Lowry Protein Assay kit (Sangon Biotechnology, China) and a phenol-concentrated sulfuric acid method, respectively.[25,26] Visualization and evaluation of biofilm thickness were performed through 3D image reconstruction using the CLSM Z-stacks function (LSM 800 with Airyscan, Carl Zeiss, Germany).[27] The biofilms were also characterized with scanning electron microscopy, as detailed in Text S7.

2.4. Determination of Biofilm Antibiotic Resistance. The biofilm samples in the culture device were removed with a sterilized scraper and resuspended in a 10 mL centrifuge tube with 0.01 M PBS. Biofilm concentration was adjusted to 10^9 CFU/mL. A sterilized bacteriostatic ring was inserted into a prepared LB agar plate, and a series of gradient concentrations (4, 8, 16, 32, 64, 128, 256, 512, and 1280 ppm) of CTX and polymyxin B (PB) were added to the bacteriostatic ring using sterilized LB culture medium as diluent. The biofilm sample was then placed in each ring. Three parallel experiments were performed with the same concentrations of antibiotics. The plates were cultured overnight at 37 °C and imaged on a gel imager system (Gel Doc XR, Bio-Rad, USA). The diffusion ability of biofilm in the antibiotic ring according to the gradient antibiotic concentration was used as the basis of antibiotic resistance. This was an original method for measuring biofilm resistance to antibiotics in our laboratory, combined with previous methods.[28]

2.5. Evaluation of Oxidative Stress in Bacterial Biofilm. Determination of bacterial intracellular reactive oxygen species (ROS) in biofilms was carried out by using the fluorescence probe method. First, 1 mL of biofilm was taken from a biofilm culture device, and 1 μL of 1 mM dichlorodihydrofluorescein diacetate (Beyotime Biotechnology, China) was added. The mixture was incubated at 37 °C for 30 min in a constant temperature incubator and mixed every 5 min. The mixture was then rinsed with PBS and resuspended into 1 mL PBS. The fluorescence intensities of the sample at 525 nm and the excitation wavelength at 488 nm were measured in a 96-well plate using a microplate analyzer

https://doi.org/10.1021/acsestwater.4c00603
ACS EST Water 2025, 5, 1546−1556

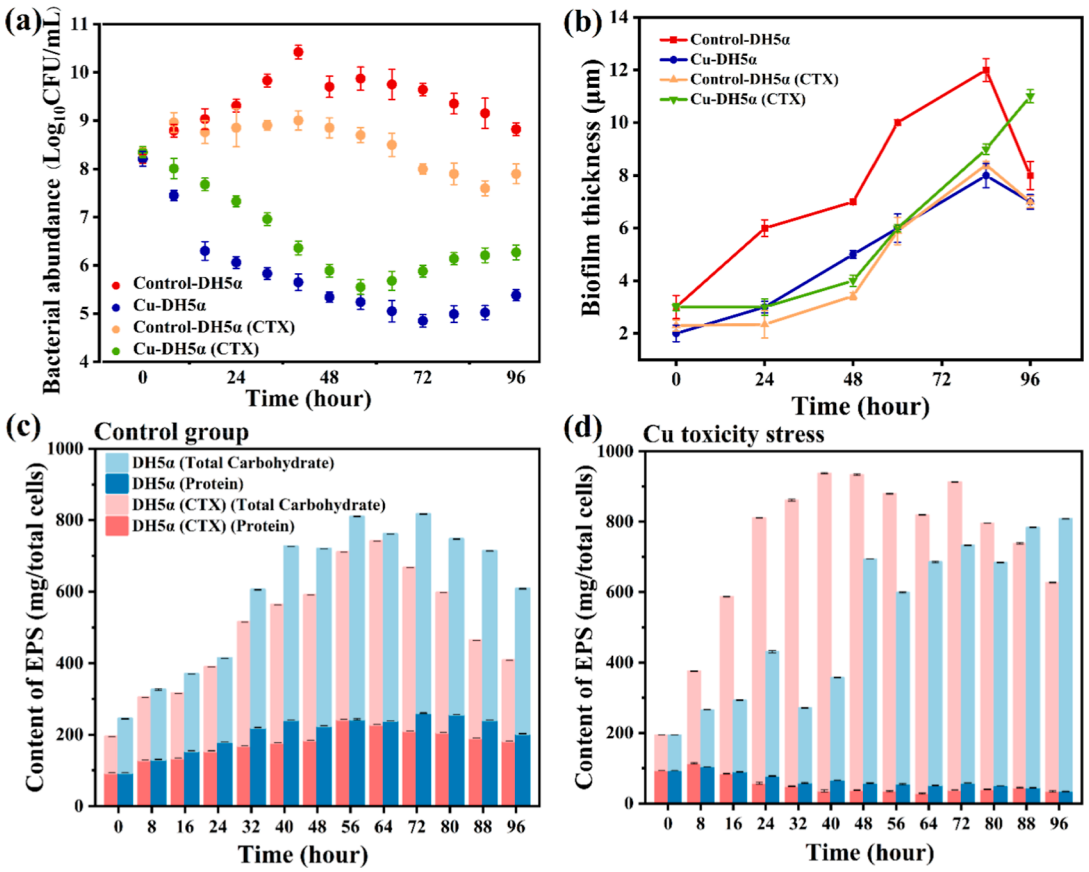

Figure 1. Growth condition of biofilm formed by *E. coli* DH5α and *E. coli* DH5α (CTX) on copper substrate and blank group. (a) The change of bacterial abundance in biofilm with culture time; (b) the change of biofilm thickness with culture time; (c) the change of EPS content under blank group with culture time; (d) the change of EPS content under cooper substrate with culture time.

(Varioskan Lux, Thermo Fisher, USA).[25,29] The activities of superoxide dismutase (SOD), catalase (CAT), and glutathione peroxidase (GSH-Px) were determined with SOD, CAT, and GSH-Px assay kits (Beyotime Biotechnology, China); the detailed steps are provided in Text S8.

2.6. Differential Gene Expression Analysis. Biofilms at different culture times were collected, washed with PBS, and stored at −80 °C until the RNA was extracted. Biofilms cultured for 0 h (planktonic bacteria) were selected as an abiotic control. The detailed steps for RNA extraction, purification, sequencing, reverse transcription, quantitative real-time polymerase chain reaction (qPCR) validation, and statistical analysis are provided in Text S9. The expression of genes related to efflux pumps, biofilm growth, and oxidative stress was also measured. Primers for all genes were designed by Sangon Biotech (Shanghai, China) and are listed in Table S2.

2.7. Statistical Analyses. All experiments were performed in at least in triplicate. All data are expressed as the means ± SD, and significant differences were determined by an independent *t*-test or one-way analysis of variance ($p < 0.05$). The laser confocal image *Z*-axis data and image pixels were converted to 3D and the parameters were analyzed using quantitative software (Imaris version 8.3, Bitplane AG, Zurich, Switzerland).[13]

3. RESULTS AND DISCUSSION

3.1. Fitness Cost of ARB Biofilms Varied in Different Environments. To explore the difference in biofilm formation mechanisms between ASB (*E. coli* DH5α) and ARB (*E. coli* DH5α (CTX)) on a copper substrate, their biofilm growth was compared with that on a quartz substrate (blank). For a given bacterium (ASB or ARB), biofilm grown on copper substrate was generally 10^2−10^5 times lower than that in the control (Figure 1a), indicating that copper substrate does inhibit biofilm growth similar to stainless steel, titanium sheet, and nickel foam.[13] However, the bacterial abundance trends were different between strains. In the control, bacterial abundance in the *E. coli* DH5α biofilm was $10^{0.5}$−$10^{1.2}$-fold higher than that in the *E. coli* DH5α (CTX) biofilm (Figure 1a). In contrast, under copper stress, bacterial abundance in the *E. coli* DH5α (CTX) biofilm was $10^{0.5}$−$10^{1.0}$ times higher than that of *E. coli* DH5α (Figure 1a). This indicates that ARB biofilms grew better under toxicity stress, while ASB biofilms grew better in the control.

Based on our previous study, ARB are more resistant to environmental stimuli because they contain ARGs.[30] However, Andersson and Hughes[17] have mentioned that plasmids carrying ARGs will bring fitness costs to bacteria carrying them, resulting in decreasing growth rates. Combining previous research and the present results, it can be concluded that the fitness cost is relative to the environment in which it is measured. In harsh environments, such as oxidative stimulation, ARGs will help bacteria better resist adverse environmental stimuli and form biofilms. However, in less stressful environments, antibiotic resistance plasmids carrying ARGs bring fitness costs and lead to the slow growth of ARB biofilms.

https://doi.org/10.1021/acsestwater.4c00603
ACS EST Water 2025, 5, 1546−1556

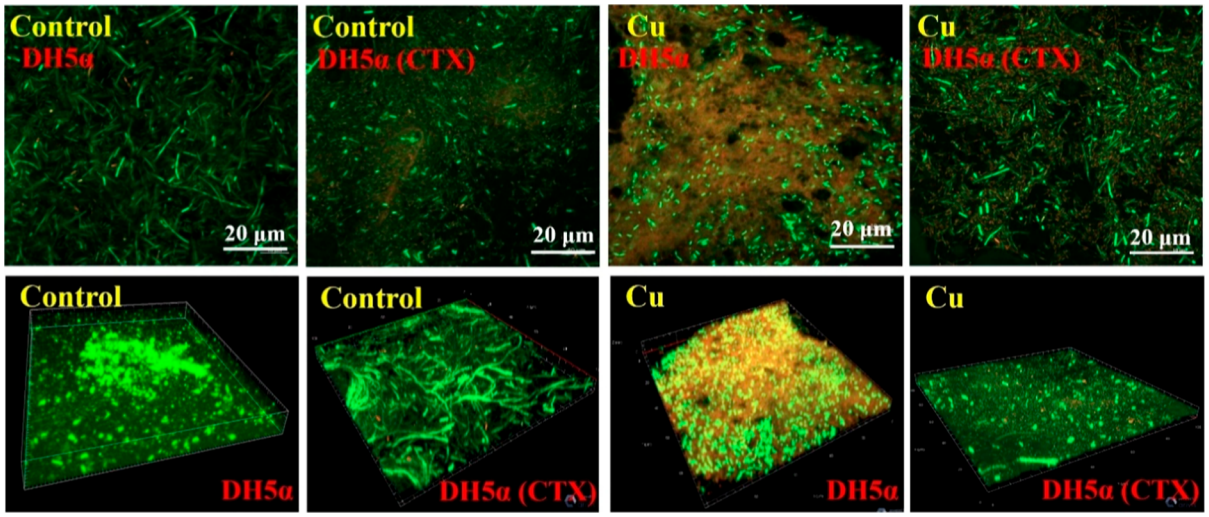

Figure 2. CLSM images showed 3D imaging of *E. coli* DH5α biofilm and *E. coli* DH5α (CTX) biofilm under the copper substrate and control group. The biofilm was stained with SYTO 9 and propidium iodide from the LIVE/DEAD BacLight kit. The green and red colors represent the lived and dead cells, respectively (the STYO 9-stained living bacteria emit green light when excited by a 488 nm laser line, and PI-stained dead bacteria emit red light when excited by a 560 nm laser line). The scale bar represents 20 μm.

Biofilms are a microbial community embedded in EPS,[31,32] which is an important part of biofilm secreted by bacterial cells,[33] making up 50%−90% of biofilms.[34] EPS content differs widely in different biofilms. In this study, the *E. coli* DH5α (CTX) biofilm was thicker under the toxicity stress of copper substrate, while the *E. coli* DH5α biofilm was thicker in the blank control (Figure 1b). The change in EPS content was consistent with this finding, as were changes in bacterial abundance (Figure 1c,d). These results further confirmed that the fitness cost of ARB biofilm and ASB biofilm growth was relative. Biofilm thickness of *E. coli* DH5α and *E. coli* DH5α (CTX) increased with prolonged culture time under copper toxicity stress (Figure 1b), consistent with previous results on biofilm growth.[20] To more intuitively determine growth differences in ARB biofilm and ASB biofilm, changes in the biofilms of *E. coli* DH5α and *E. coli* DH5α (CTX) on copper substrate and control substrates were further visualized with 3D CLSM; these results were consistent with those seen above (Figure S5).

The ratio of carbohydrate to protein also plays an important role in detecting the formation of biofilm.[35,36] A more intuitive figure of the changes in bacterial abundance and the ratio of total carbohydrate/protein was also drawn. Under toxicity stress of copper substrate, polysaccharide content increased and protein content remained almost unchanged with increasing culture time (Figure S6), further leading to the increase of the ratio of total carbohydrate to protein. This might be because when they touch and attach to the copper substrate surface, some bacteria will be killed dynamically.[10] Because of this, total carbohydrates in measured EPS might also include cell fragments, which could be detected through the filter membrane, resulting in high levels of carbohydrates (Figure 1d). The protein content remained unchanged (30−50 mg/total cells), indicating that protein content leaked from broken cells was almost negligible compared with protein content of EPS secreted by biofilm (Figure 1d). The dynamic characteristics of EPS in biofilm depend on its water demand.[37] This result further demonstrated that ASB biofilm had more difficulty adapting to the toxicity stress of copper substrate than that of ARB, probably due to the ARG carried by *E. coli* DH5α (CTX) as an enhanced gene to help ARB biofilm resist the stress of copper substrate.

The live and dead bacteria in the biofilms were imaged with 3D CLSM after the biofilms were dyed (Figure 2). More dead bacterial cells (bacteria dyed red) in the biofilms were observed on copper substrate than on the blank control group. On the copper substrate, more bacterial cells died in the *E. coli* DH5α biofilm than in the *E. coli* DH5α (CTX) biofilm, opposite to the results of the control. This further confirmed that ARB biofilm was more adaptable to harsh conditions than ASB biofilm, which was more adaptable to environmental conditions without stress. This also verified the correctness of the above conclusions and further indicates that ARGs act as an enhanced gene resistance to harsh environments under the toxicity stress of copper substrate, though it has a certain fitness cost in a blank environment.

3.2. Toxicity Stress of Copper Substrate Increased Biofilm Antibiotic Resistance. Bacteria in the biofilm state have higher antibiotic resistance capability than in the planktonic state.[38,39] The results also showed that the fitness costs of ARB biofilm and ASB biofilm under copper substrate toxicity stress were different from those in the control (Figures 1 and 2). To clarify whether the changes in antibiotic resistance of ARGs still have the same fitness costs as growth activity, the antibiotic resistance of biofilms was further characterized. The changes in biofilm resistance to CTX and PB were measured first (the action mechanism of these antibiotics is shown in Table S3 and Figure 3a).

As expected, the *E. coli* DH5α (CTX) biofilm universally had higher antibiotic resistance than the *E. coli* DH5α biofilm, both in the control and on the copper substrate (Figure 3b). The different growth trends (Figure 1) had no obvious association with fitness costs for the antibiotic resistance of ARGs to biofilms (Figure 3b). A similar conclusion was reached when determining bacterial efflux pump-related gene abundance (*aaeX*, *acrB*, and *acrD*) in biofilms (Figure S7). With the blank substrate and toxicity stress of the copper substrate, *E. coli* DH5α (CTX) biofilm had higher antibiotic resistance not only to CTX but also to PB than did *E. coli* DH5α biofilm (Figure 3b), indicating that high resistance of *E.*

https://doi.org/10.1021/acsestwater.4c00603
ACS EST Water 2025, 5, 1546−1556

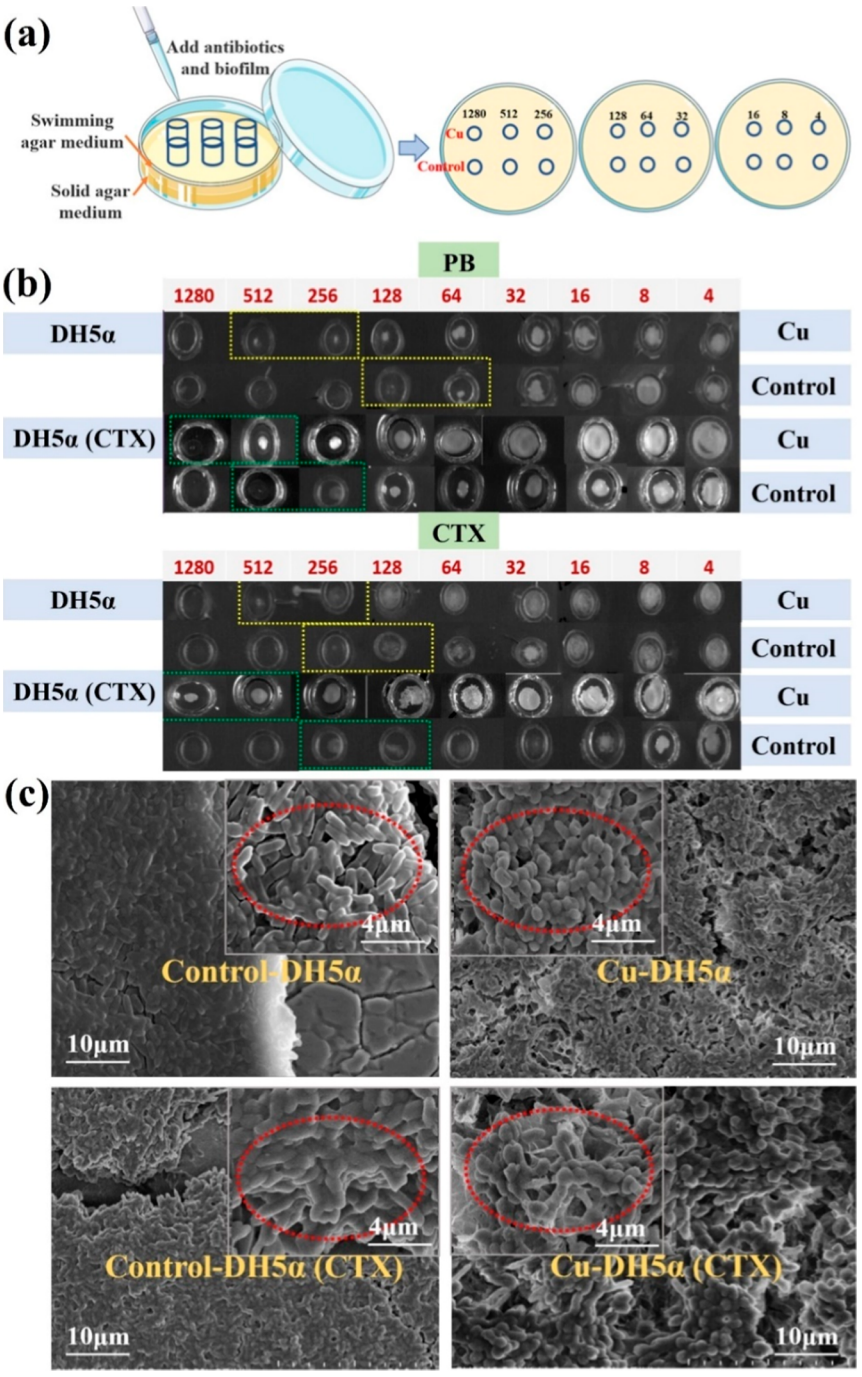

Figure 3. (a) Experimental design and method diagram for characterization of antibiotic resistance biofilm; (b) determination of resistance of biofilm formed by *E. coli* DH5α and *E. coli* DH5α (CTX) under copper substrate and blank conditions to antibiotics CTX and PB (gel imaging map); (c) the SEM images of *E. coli* DH5α biofilm and *E. coli* DH5α (CTX) biofilm cultured on copper substrate and blank group.

coli DH5α (CTX) biofilm to universal antibiotics was not due to the existence of the $bla_{ctx\text{-}1}$ gene. This may explain why there were so many factors influencing the mechanisms of antibiotic resistance in biofilms, as other more important factors eliminate differences in their fitness costs. Changes in biofilm antibiotic resistance are related to the barrier ability of biofilm.[25] Although antibiotic resistance between the ARB biofilm and ASB biofilm did not have different fitness costs with either the copper substrate or control, it does not mean that they did not produce corresponding fitness costs. Further research is required on whether the fitness costs exist and whether they can affect antibiotic resistance changes in biofilms.

There appeared to be no obvious fitness costs of ARGs to biofilm resistance for both kinds of bacteria, although the biofilm grown on copper substrate was more resistant to antibiotics than that of the blank group (Figure 3b). To further explain the intrinsic reasons behind the stronger antibiotic resistance of biofilms grown on copper substrate, the morphological changes of biofilms were observed. The morphology of bacteria in biofilm formed on copper substrate changed, with *E. coli* DH5α (CTX) or *E. coli* DH5α becoming short rod-shaped or even spherical cells (Figure 3c). This

https://doi.org/10.1021/acsestwater.4c00603
ACS EST Water 2025, 5, 1546−1556

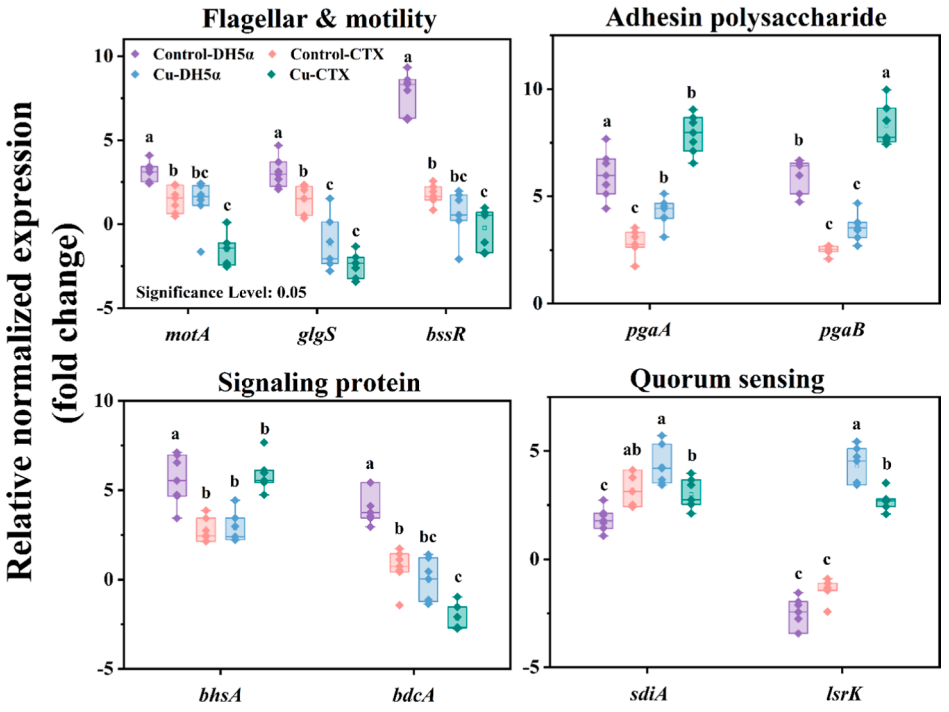

Figure 4. Log_2 fold changes of target genes involved in flagellar and motility, adhesin polysaccharide, signaling protein, and QS system in *E. coli* DH5α biofilm and *E. coli* DH5α (CTX) biofilm in blank control group and copper substrate group. The different lowercase letters represent significant differences between groups (Tukey's HSD test, $p < 0.05$). Control group: control-*E. coli* DH5α.

might be because bacteria can become persistent, becoming viable but nonculturable cells (VBNC) or small colony variants (SCVs).[40] The changes in physiological morphology are thought to occur because they are under stress from an adverse environment. *E. coli* cells, for example, become shorter after treatment with chlorine and chloramine.[41,42] Under environmental stimulation, bacteria enter VBNC, SCV, or other persistent states to cope with changes in the water environment.[43] Bacteria in these dormant states are more tolerant to environmental stimulation, which also explains why the antibiotic resistance in biofilms increased under copper substrate toxicity stress.

3.3. Antibiotic-Resistant Biofilms Better Adapted to Substrate Toxicity Stress. When bacteria are subjected to harmful stimulation, they will produce high levels of highly active molecules such as intracellular ROS, resulting in an imbalance between oxidation and the antioxidant system.[44] For the antioxidant system, specific enzymes, including SOD, CAT, and GSH-Px, will be produced when bacteria are subjected to oxidative stress.[45] In this study, the intracellular ROS content of *E. coli* DH5α grown on copper substrate was 1.1−1.2 times higher than that of *E. coli* DH5α (CTX) (Figure S8a), indicating that ARB are more adaptable to the toxicity stress of copper substrate. These results can explain the underlying causes of the higher growth and fewer dead bacteria seen in the *E. coli* DH5α (CTX) biofilm (Figures 1 and 2). In contrast, for the blank control, the intracellular ROS levels of *E. coli* DH5α (CTX) were 1.1−1.3 times higher than that of *E. coli* DH5α. This also further indicates that under blank conditions antibiotic resistance plasmids carrying ARGs place a fitness burden on bacteria, exposing them to oxidative stress (Figure S8a). The content changes in related antioxidant enzymes showed the same trends as intracellular ROS content, further explaining the changes in the level of oxidative stress (Figure S8a). These results explained the intrinsic reasons why *E. coli* DH5α (CTX) showed different adaptability to different environments (Section 3.1), further demonstrating the fitness cost of ARGs in terms of oxidative stress.

To further confirm the oxidative stress in biofilm bacteria and clarify the interactions between biofilms and copper substrate during biofilm formation, the expression of oxidative stress- (*osmC*, *soxR*, *ompR*, *sodA*, *oxyR*, *yiaA*, and *rpoS*) and metal transporter (*zupT*, *fieF*, and *zinT*)-related genes was measured. In the blank control, the expression of oxidative stress-related genes in *E. coli* DH5α (CTX) biofilm was up-regulated by 0.5−6.7 fold, higher than that in the *E. coli* DH5α biofilm (−3.8 to 4.8 fold change) (negative value indicating down-regulation) (Figure S8e). These results showed that under no environmental selection pressure, the antibiotic resistance plasmid of *E. coli* DH5α (CTX) posed a burden, subjecting cells to strong oxidative stress during biofilm growth, which caused fitness costs, resulting in slow growth. This explained why the ARB biofilm had more fitness costs to growth than the ASB biofilm under the control conditions (Section 3.1; Figures 1 and 2). The highly expressed *soxR* and *oxyR* genes encode two transcriptional activators that regulate the oxidative stress defense mechanism; they further induce the expression of genes related to membrane repair (*yiaA*), DNA repair (*rpoS*), and the SOS response (*ompR*).[44]

Under copper substrate toxicity stress, the expression of oxidative stress-related genes in the *E. coli* DH5α biofilm was up-regulated by 1.2−10.2 fold, much higher than that in the *E. coli* DH5α (CTX) biofilm (−0.9 to 4.9 fold changes) (Figure S8e). These results demonstrate that under the stress of the copper substrate, the ARG (bla_{ctx-1}) in *E. coli* DH5α (CTX) helped the cells resist adverse environmental stimuli, reducing their oxidative stress response. The expression of metal transporter-related genes (*zupT*, *fieF*, and *zinT*) in *E. coli*

https://doi.org/10.1021/acsestwater.4c00603
ACS EST Water 2025, 5, 1546−1556

DH5α (CTX) was also significantly lower than that in *E. coli* DH5α on a copper substrate. The expression of metal transporter-related genes would cause the Cu surface to be oxidized to Cu^{2+}, which could then enter bacterial cells through metal transporters, resulting in intracellular redox imbalance and compromising cell membrane permeability.[46] These findings indicated that the $bla_{ctx\text{-}1}$ gene in the *E. coli* DH5α (CTX) biofilm inhibited metal transporter expression. Overall, these results explained the intrinsic reasons behind how ARGs both help bacteria resist adverse environmental stimuli and bring fitness costs.

3.4. Antibiotic-Resistant Biofilm Had Better Fitness under Copper Substrate Stress due to c-di-GMP Activated Signaling. The expression of genes related to biofilm growth was further measured to explore how the $bla_{ctx\text{-}1}$ gene enhanced genes, facilitating bacterial resistance to adverse stimuli. Biofilm growth is related to many factors, including flagellar motility, quorum sensing (QS), and c-di-GMP signaling.[47−49] The expression of genes related to flagella and motility, (*motA*, *glgS*, and *bssR*), polysaccharide synthesis (*pgaA* and *pgaB*), c-di-GMP signaling (*bhsA* and *bdcA*), and QS (*sdiA* and *lsrK*) was measured after 72 h of biofilm growth.

In the blank control, the expression of *motA* and *bssR* in *E. coli* DH5α (CTX) biofilm was up-regulated by 0.5−2.6 fold, while that in *E. coli* DH5α biofilm was up-regulated by 2.4−9.3 fold (Figure 4). This indicated that after 72 h of biofilm growth, flagella production and bacterial motility in ASB biofilm were more active, indicating that it may grow better than ARB biofilm. The biofilm is at the growth and maturity stage after 72 h of culture, at which biofilm thickness, bacterial abundance, and EPS content reach their highest values.[25] When the biofilm growth enters the dispersion stage, the flagella of bacteria regrow and cell motility increases.[50] The *glgS* gene is related to glycogen synthesis and negative motility regulation.[13] Expression of this gene was also up-regulated at 72 h of culture (Figure 4). This indicated that flagellar motility had not been completely regulated at this time, indicating that the biofilm had not yet completely entered the dispersion stage. These conclusions further explained why the growth of ASB biofilm was higher than that of ARB biofilm (Section 3.1).

As EPS is an important component of biofilm, and polysaccharides are an important component of EPS,[34] expression of genes related to polysaccharide synthesis in *E. coli* DH5α (CTX) and *E. coli* DH5α was further measured (Figure 4). The specific up-regulation of genes related to biofilm growth of *E. coli* DH5α (3.4−7.6 fold) was higher than that in the ARB *E. coli* DH5α (CTX) (0.7−2.8 fold) in the blank control, further explaining the higher growth of ASB (Section 3.1) from the level of molecular regulation.

Biofilm formation-related gene expression was further analyzed under copper stress. The gene related to c-di-GMP signaling (*bhsA*) was up-regulated more (4.7−7.7 fold) than other QS-related genes such as *sdiA* and *lsrK* (2.1−3.9 fold) on copper substrate. The *bhsA* gene of *E. coli* DH5α (CTX) biofilm was up-regulated by 4.7−7.7 fold, while that in the *E. coli* DH5α biofilm was only up-regulated by 2.2−4.4 fold (Figure 4). The transition from planktonic bacteria to biofilm formation is characterized by a series of physiological, metabolic, and phenotypic changes, which are coordinated with secondary messenger c-di-GMP.[49] Elevated concentration of c-di-GMP induces biofilm formation, while low concentration of c-di-GMP causes biofilm dispersion.[50] Under the toxicity stress of copper substrate, the *bdcA* gene down-regulated for both bacterial strains, although the down-regulation of the *bdcA* gene for *E. coli* DH5α (CTX) was more obvious than that for *E. coli* DH5α (Figure 4). These results further indicate that *E. coli* DH5α (CTX) grows better than *E. coli* DH5α under the toxicity stress of the copper substrate. It is because *bdcA* is a gene regulating biofilm diffusion, inhibiting its expression is beneficial to biofilm formation.[50]

The expression of the QS-related gene *sdiA* in *E. coli* DH5α (CTX) and *E. coli* DH5α was also up-regulated by 4.4- and 3.0-fold, respectively (Figure 4). The protein encoded by *sdiA* is a receptor for QS signal molecules.[48] These results further indicate that QS signal molecules are produced in both ARB and ASB during biofilm formation on a copper substrate, which promotes the synthesis of receptor protein encoded by *sdiA*. Another gene associated with the QS system, *lsrK*, encodes the phosphorylated kinase of self-inducing conductor autoinducer 2 (AI-2).[51] In the blank control, the expression of *lsrK* was down-regulated both in *E. coli* DH5α (CTX) biofilm (−2.4 to 0.3 fold) and *E. coli* DH5α biofilm (−3.4 to 0.5 fold). This may be caused by the formation of a mature biofilm; decreases in QS signal AI-2 molecules usually occur in mature biofilms, inhibiting *lsrK* gene expression[52] and reducing the synthesis of AI-2 (Figure 4). Comparatively, under the toxicity stress of copper substrate, the expression of *lsrK* was up-regulated both in *E. coli* DH5α (CTX) biofilm (2.1−3.5 fold) and *E. coli* DH5α biofilm (3.4−6.7 fold), indicating that bacteria were in an active stress state under the toxicity stress of copper substrate, and up-regulation of *lsrK* helped bacterial aggregation to promote biofilm formation (Figure 4). This result indicates that at the mature stage of biofilm growth, the *lsrK* gene is down-regulated to inhibit biofilm formation, while when biofilm formation is stimulated, its expression is up-regulated to promote biofilm formation. Under copper stress, the up-regulation of *lsrK* in *E. coli* DH5α (3.4−6.7 fold) was higher than that in *E. coli* DH5α (CTX) (2.1−3.5 fold). This also indicated that, compared with the ASB biofilm, the ARB biofilm was more adaptable to the toxicity stress of the copper substrate.

Combined with the expression of oxidative stress-related genes (Figure S8b) and biofilm growth-related genes (Figure 4) under the toxicity stress of copper substrate, the expression of biofilm growth-related genes in the *E. coli* DH5α (CTX) biofilm was significantly higher than that of oxidative stress-related genes. This indicates that although copper substrate toxicity stress improved the expression of biofilm growth-related genes and bacterial abundance, biofilm thickness, and EPS content in the *E. coli* DH5α (CTX) biofilm, this effect was not mainly caused by oxidative stress. When bacteria are stimulated by environmental conditions (such as phthalate esters released from plastics and low concentrations of polyvalent bacteriophages), biofilm formation occurs due to the promotion of oxidative stress.[47,53] However, the results showed that the oxidative stress response of the *E. coli* DH5α (CTX) biofilm (including intracellular ROS content and the concentration of the antioxidant enzymes SOD, CAT, and GSH-Px) increased under the toxicity stress from the copper substrate, but not as much as that of the *E. coli* DH5α biofilm. This was confirmed by the expression measurements of oxidative stress-related genes (Figure S8a,b). These results show that another signaling pathway that was more important than the oxidative stress signal pathway led to biofilm formation in the ARB under copper substrate toxicity stress.

https://doi.org/10.1021/acsestwater.4c00603
ACS EST Water 2025, 5, 1546−1556

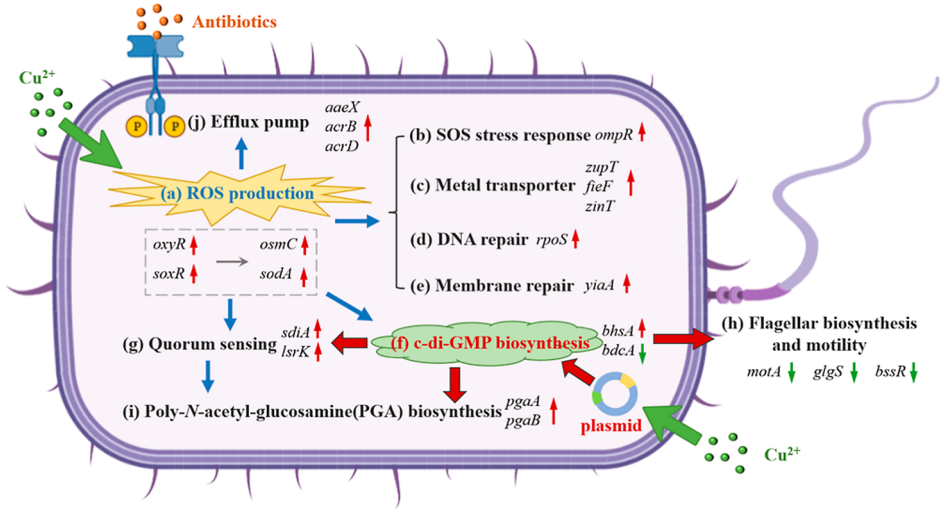

Figure 5. Response mechanism during biofilm formation of DH5α (CTX) under the stress of copper substrate.

The c-di-GMP signaling plays a significant role in biofilm formation.[49,54] On copper substrate, the *bhsA* gene associated with c-di-GMP signaling in *E. coli* DH5α (CTX) was up-regulated much higher (4.7−7.7 fold) than that of *E. coli* DH5α (2.2−4.4 fold) (Figure 4). It can be concluded that under the toxicity stress from the copper substrate, the biofilm formation of ARB was dominated by c-di-GMP signaling rather than signaling activated by intracellular ROS. This led to better adaptation of the ARB biofilm to the harsh environment, resulting in better biofilm formation. The specific signal pathways are demonstrated in detail in Figure 5. The intracellular c-di-GMP concentration of bacteria in biofilms after 72 h of culture was measured with an enzyme-linked immunosorbent assay, further supporting this conclusion. The specific operation of c-di-GMP determination is shown in Text S10, and the results are shown in Figure S9.

This study emphasizes the potential for ARB spread and the formation of ARB biofilms in water supply and heating systems using copper products. ARB are more capable of surviving under the environmental stress imposed by copper than ASB. This raises concerns about the potential for copper products to contribute to the proliferation of ARB and increase the risk of their spread, posing potential risks to people who rely on water sources outfitted with copper. Although M9 low salt broth was used in this study to maximize the simulation of the real water supply environment, it is important to note that this study was conducted under controlled laboratory conditions and real-world outcomes may differ. Also, the long-term monitoring and assessment of the colonization of ARB in actual water supply systems is necessary. Additionally, various factors in actual pipelines could cause fluctuations in the concentration of copper ions, affecting biofilm growth. However, in this work, the effect of the copper ion concentration on biofilm growth was not assessed. It is important to further explore the growth differences of ARB biofilms under different copper ion concentrations in the future. Despite these limitations, this study provides valuable insights for future research into the colonization of ARB biofilms in copper pipes in real-world settings.

4. CONCLUSIONS

This study mainly revealed the differences in biofilm growth on copper substrate between ASB and ARB. The biofilm carrying antibiotic resistance plasmids grew better than the antibiotic-sensitive biofilm on the copper substrate due to ARGs, which enabled bacteria to resist adverse environmental conditions. The biofilm formed by ARB had higher bacterial abundance, larger thickness, and higher EPS concentration than that of ASB on the copper substrate. ARB biofilms also had lower oxidative stress levels and were better adapted to the copper substrate. The biofilm formation of ARB was primarily triggered by the signal pathway activated by c-di-GMP, rather than the SOS signal pathway activated by intracellular ROS. In conclusion, although further study is needed to determine whether there is a fitness cost associated with antibiotic resistance, the findings of this study help us to understand ARB biofilm colonization on copper substrates. This can aid in avoiding the selection of copper products in water supply and heating systems to reduce the growth of ARB biofilms and the spread of antibiotic resistance.

■ ASSOCIATED CONTENT

Supporting Information

The Supporting Information is available free of charge at https://pubs.acs.org/doi/10.1021/acsestwater.4c00603.

Experimental details; primers of genes used for RT-PCR assays; the action mechanism of two classes of antibiotics; schematic diagram of *E. coli* DH5α (CTX) construction; photos and schematic diagram of a multichannel biofilm flow chamber; the photos of copper substrate; the SEM images of copper substrate; the XRD result of copper substrate; CLSM imaging revealed the growth change condition of *E. coli* DH5α biofilm and *E. coli* DH5α (CTX) biofilm on copper substrate and the blank control group with different culture time; changes of the ratio of carbohydrate and protein content in EPS of biofilms; and expression levels of genes (PDF)

■ AUTHOR INFORMATION

Corresponding Author

Taicheng An − *Guangdong Key Laboratory of Environmental Catalysis and Health Risk Control, Guangdong-Hong Kong-Macao Joint Laboratory for Contaminants Exposure and Health, Institute of Environmental Health and Pollution*

https://doi.org/10.1021/acsestwater.4c00603
ACS EST Water 2025, 5, 1546−1556

Control, Guangdong University of Technology, Guangzhou 510006, China; Guangzhou Key Laboratory of Environmental Catalysis and Pollution Control, Guangdong Technology Research Center for Photocatalytic Technology Integration and Equipment Engineering, School of Environmental Science and Engineering, Guangdong University of Technology, Guangzhou 510006, China; orcid.org/0000-0001-6918-8070; Email: antc99@gdut.edu.cn

Authors

Min Chen − *Guangdong Key Laboratory of Environmental Catalysis and Health Risk Control, Guangdong-Hong Kong-Macao Joint Laboratory for Contaminants Exposure and Health, Institute of Environmental Health and Pollution Control, Guangdong University of Technology, Guangzhou 510006, China; Guangzhou Key Laboratory of Environmental Catalysis and Pollution Control, Guangdong Technology Research Center for Photocatalytic Technology Integration and Equipment Engineering, School of Environmental Science and Engineering, Guangdong University of Technology, Guangzhou 510006, China*

Jiaping Wang − *Guangdong Key Laboratory of Environmental Catalysis and Health Risk Control, Guangdong-Hong Kong-Macao Joint Laboratory for Contaminants Exposure and Health, Institute of Environmental Health and Pollution Control, Guangdong University of Technology, Guangzhou 510006, China; Guangzhou Key Laboratory of Environmental Catalysis and Pollution Control, Guangdong Technology Research Center for Photocatalytic Technology Integration and Equipment Engineering, School of Environmental Science and Engineering, Guangdong University of Technology, Guangzhou 510006, China*

Longji Xia − *Guangdong Key Laboratory of Environmental Catalysis and Health Risk Control, Guangdong-Hong Kong-Macao Joint Laboratory for Contaminants Exposure and Health, Institute of Environmental Health and Pollution Control, Guangdong University of Technology, Guangzhou 510006, China; Guangzhou Key Laboratory of Environmental Catalysis and Pollution Control, Guangdong Technology Research Center for Photocatalytic Technology Integration and Equipment Engineering, School of Environmental Science and Engineering, Guangdong University of Technology, Guangzhou 510006, China*

Guiying Li − *Guangdong Key Laboratory of Environmental Catalysis and Health Risk Control, Guangdong-Hong Kong-Macao Joint Laboratory for Contaminants Exposure and Health, Institute of Environmental Health and Pollution Control, Guangdong University of Technology, Guangzhou 510006, China; Guangzhou Key Laboratory of Environmental Catalysis and Pollution Control, Guangdong Technology Research Center for Photocatalytic Technology Integration and Equipment Engineering, School of Environmental Science and Engineering, Guangdong University of Technology, Guangzhou 510006, China;* orcid.org/0000-0002-6777-4786

Wanjun Wang − *Guangdong Key Laboratory of Environmental Catalysis and Health Risk Control, Guangdong-Hong Kong-Macao Joint Laboratory for Contaminants Exposure and Health, Institute of Environmental Health and Pollution Control, Guangdong University of Technology, Guangzhou 510006, China; Guangzhou Key Laboratory of Environmental Catalysis and Pollution Control, Guangdong Technology Research Center for Photocatalytic Technology Integration and Equipment Engineering, School of Environmental Science and Engineering, Guangdong University of Technology, Guangzhou 510006, China;* orcid.org/0000-0003-1193-1030

Complete contact information is available at: https://pubs.acs.org/10.1021/acsestwater.4c00603

Author Contributions

[§]M.C. and J.W. authors contributed equally to this work.

Notes

The authors declare no competing financial interest.

■ ACKNOWLEDGMENTS

This work was supported by the National Natural Science Foundation of China (42330702) and the Key Project of Guangdong-Guangxi Joint Fund (2020B1515420002).

■ REFERENCES

(1) Ma, L.; Jiang, X. T.; Guan, L.; Li, B.; Zhang, T. Nationwide biogeography and health implications of bacterial communities in household drinking water. *Water Res.* **2022**, *215*, 118238.

(2) Wee, S. Y.; Aris, A. Z. Occurrence and public-perceived risk of endocrine disrupting compounds in drinking water. *npj Clean Water* **2019**, *2*, 4.

(3) Ardal, C.; Balasegaram, M.; Laxminarayan, R.; McAdams, D.; Outterson, K.; Rex, J. H.; Sumpradit, N. Antibiotic development - economic, regulatory and societal challenges. *Nat. Rev. Microbiol.* **2020**, *18*, 267−274.

(4) Zhang, J.; Xu, Z.; Chu, W.; Ju, F.; Jin, W.; Li, P.; Xiao, R. Residual chlorine persistently changes antibiotic resistance gene composition and increases the risk of antibiotic resistance in sewer systems. *Water Res.* **2023**, *245*, 120635.

(5) Fu, Y.; Peng, H.; Liu, J.; Nguyen, T. H.; Hashmi, M. Z.; Shen, C. Occurrence and quantification of culturable and viable but non-culturable (VBNC) pathogens in biofilm on different pipes from a metropolitan drinking water distribution system. *Sci. Total Environ.* **2021**, *764*, 142851.

(6) Tang, W.; Li, Q.; Chen, L.; Zhang, W.-x.; Wang, H. Biofilm community structures and opportunistic pathogen gene markers in drinking water mains and the role of pipe materials. *ACS ES&T Water* **2021**, *1*, 630−640.

(7) Learbuch, K. L. G.; Smidt, H.; van der Wielen, P. Influence of pipe materials on the microbial community in unchlorinated drinking water and biofilm. *Water Res.* **2021**, *194*, 116922.

(8) Song, Y.; Pruden, A.; Edwards, M. A.; Rhoads, W. J. Natural organic matter, orthophosphate, pH, and growth phase can limit copper antimicrobial efficacy for *Legionella* in drinking water. *Environ. Sci. Technol.* **2021**, *55*, 1759−1768.

(9) Martin, R. L.; Strom, O.; Song, Y.; Mena-Aguilar, D.; Rhoads, W. J.; Pruden, A.; Edwards, M. A. Copper pipe, lack of corrosion control, and very low pH may have influenced the trajectory of the flint Legionnaires' disease outbreak. *ACS ES&T Water* **2022**, *2*, 1440−1450.

(10) Li, Q.; Xu, X.; Li, W.; Wang, G. Complexation of copper algicide and cellular organic matter: implications for its fate in algae-laden surface waters. *ACS ES&T Water* **2023**, *3*, 2286−2295.

(11) Jeanvoine, A.; Meunier, A.; Puja, H.; Bertrand, X.; Valot, B.; Hocquet, D. Contamination of a hospital plumbing system by persister cells of a copper-tolerant high-risk clone of Pseudomonas aeruginosa. *Water Res.* **2019**, *157*, 579−586.

(12) Levin-Reisman, I.; Ronin, I.; Gefen, O.; Braniss, I.; Shoresh, N.; Balaban, N. Q. Antibiotic tolerance facilitates the evolution of resistance. *Science* **2017**, *355* (6327), 826−830.

(13) Wang, J.; Li, G.; Yin, H.; An, T. Bacterial response mechanism during biofilm growth on different metal material substrates: EPS characteristics, oxidative stress and molecular regulatory network analysis. *Environ. Res.* **2020**, *185*, 109451.
(14) Lewis, K. The science of antibiotic discovery. *Cell* **2020**, *181*, 29−45.
(15) Balaban, N. Q.; Helaine, S.; Lewis, K.; Ackermann, M.; Aldridge, B.; Andersson, D. I.; Brynildsen, M. P.; Bumann, D.; Camilli, A.; Collins, J. J.; Dehio, C.; Fortune, S.; Ghigo, J. M.; Hardt, W. D.; Harms, A.; Heinemann, M.; Hung, D. T.; Jenal, U.; Levin, B. R.; Michiels, J.; Storz, G.; Tan, M. W.; Tenson, T.; Van Melderen, L.; Zinkernagel, A. Definitions and guidelines for research on antibiotic persistence. *Nat. Rev. Microbiol.* **2019**, *17*, 441−448.
(16) Ciofu, O.; Moser, C.; Jensen, P. O.; Hoiby, N. Tolerance and resistance of microbial biofilms. *Nat. Rev. Microbiol.* **2022**, *20*, 621−635.
(17) Andersson, D. I.; Hughes, D. Antibiotic resistance and its cost: is it possible to reverse resistance? *Nat. Rev. Microbiol.* **2010**, *8* (4), 260−271.
(18) Rodriguez-Beltran, J.; DelaFuente, J.; Leon-Sampedro, R.; MacLean, R. C.; San Millan, A. Beyond horizontal gene transfer: the role of plasmids in bacterial evolution. *Nat. Rev. Microbiol.* **2021**, *19*, 347−359.
(19) San Millan, A.; Toll-Riera, M.; Qi, Q.; Betts, A.; Hopkinson, R. J.; McCullagh, J.; MacLean, R. C. Integrative analysis of fitness and metabolic effects of plasmids in *Pseudomonas aeruginosa* PAO1. *ISME J.* **2018**, *12*, 3014−3024.
(20) Flemming, H. C.; Wingender, J.; Szewzyk, U.; Steinberg, P.; Rice, S. A.; Kjelleberg, S. Biofilms: an emergent form of bacterial life. *Nat. Rev. Microbiol.* **2016**, *14*, 563−575.
(21) Young, S.; Rohr, J. R.; Harwood, V. J. Vancomycin resistance plasmids affect persistence of *Enterococcus faecium* in water. *Water Res.* **2019**, *166*, 115069.
(22) Abdulaziz, A.; Sathyendranath, S.; Vijayakumar, S. K.; Menon, N.; George, G.; Kulk, G.; Raj, D.; Krishna, K.; Rajamohananpillai, R.; Tharakan, B.; Jasmin, C.; Vengalil, J.; Platt, T. The distribution of fecal contamination in an urbanized tropical lake and incidence of acute diarrheal disease. *ACS ES&T Water* **2023**, *3*, 1561−1573.
(23) Rao, G.; Kahler, A.; Voth-Gaeddert, L. E.; Cranford, H.; Libbey, S.; Galloway, R.; Molinari, N.-A.; Ellis, E. M.; Yoder, J. S.; Mattioli, M. C.; Ellis, B. R. Microbial characterization, factors contributing to contamination, and household use of cistern water, U.S. Virgin Islands. *ACS ES&T Water* **2022**, *2*, 2634−2644.
(24) Stoodley, P.; Sauer, K.; Davies, D. G.; Costerton, J. W. Biofilms as complex differentiated communities. *Annu. Rev. Microbiol.* **2002**, *56*, 187−209.
(25) Chen, M.; Cai, Y.; Li, G.; Zhao, H.; An, T. The stress response mechanisms of biofilm formation under sub-lethal photocatalysis. *Appl. Catal., B* **2022**, *307*, 121200.
(26) Proctor, C. R.; Dai, D.; Edwards, M. A.; Pruden, A. Interactive effects of temperature, organic carbon, and pipe material on microbiota composition and *Legionella pneumophila* in hot water plumbing systems. *Microbiome* **2017**, *5*, 130.
(27) Stone, M. R. L.; Butler, M. S.; Phetsang, W.; Cooper, M. A.; Blaskovich, M. A. T. Fluorescent antibiotics: new research tools to fight antibiotic resistance. *Trends Biotechnol.* **2018**, *36*, 523−536.
(28) Jorge, P.; Magalhaes, A. P.; Grainha, T.; Alves, D.; Sousa, A. M.; Lopes, S. P.; Pereira, M. O. Antimicrobial resistance three ways: healthcare crisis, major concepts and the relevance of biofilms. *FEMS Microbiol. Ecol.* **2019**, *95*, fiz115.
(29) Zhang, S.; Wang, Y.; Lu, J.; Yu, Z.; Song, H.; Bond, P. L.; Guo, J. Chlorine disinfection facilitates natural transformation through ROS-mediated oxidative stress. *ISME J.* **2021**, *15*, 2969−2985.
(30) Yin, H.; Li, G.; Chen, X.; Wang, W.; Wong, P. K.; Zhao, H.; An, T. Accelerated evolution of bacterial antibiotic resistance through early emerged stress responses driven by photocatalytic oxidation. *Appl. Catal., B* **2020**, *269*, 118829.
(31) Koo, H.; Allan, R. N.; Howlin, R. P.; Stoodley, P.; Hall-Stoodley, L. Targeting microbial biofilms: current and prospective therapeutic strategies. *Nat. Rev. Microbiol.* **2017**, *15*, 740−755.
(32) Matviichuk, O.; Mondamert, L.; Geffroy, C.; Dagot, C.; Labanowski, J. Life in an unsuspected antibiotics world: River biofilms. *Water Res.* **2023**, *231*, 119611.
(33) Huang, G.; Xia, D.; An, T.; Ng, T. W.; Yip, H. Y.; Li, G.; Zhao, H.; Wong, P. K. Dual roles of capsular extracellular polymeric substances in photocatalytic inactivation of *Escherichia coli:* Comparison of *E. coli* BW25113 and isogenic mutants. *Appl. Environ. Microbiol.* **2015**, *81*, 5174−5183.
(34) Flemming, H. C.; Wingender, J. The biofilm matrix. *Nat. Rev. Microbiol.* **2010**, *8*, 623−633.
(35) Peng, S.; Hu, A.; Ai, J.; Zhang, W.; Wang, D. Changes in molecular structure of extracellular polymeric substances (EPS) with temperature in relation to sludge macro-physical properties. *Water Res.* **2021**, *201*, 117316.
(36) Cui, X.; Ren, T.; Ren, Q.; Wu, B.; Zhou, Y.; Xia, S.; Rittmann, B. E. Sensitive and accurate differentiation of extracellular polymeric substance hydrolysis using flow cytometry during biofilm extracellular polymeric substance extraction. *ACS ES&T Water* **2023**, *3*, 1019−1028.
(37) Lemus Pérez, M. F.; Rodríguez Susa, M. Exopolymeric substances from drinking water biofilms: Dynamics of production and relation with disinfection by products. *Water Res.* **2017**, *116*, 304−315.
(38) Fang, K.; Park, O. J.; Hong, S. H. Controlling biofilms using synthetic biology approaches. *Biotechnol. Adv.* **2020**, *40*, 107518.
(39) Desiante, W. L.; Minas, N. S.; Fenner, K. Micropollutant biotransformation and bioaccumulation in natural stream biofilms. *Water Res.* **2021**, *193*, 116846.
(40) Cai, Y.; Liu, J.; Li, G.; Wong, P. K.; An, T. Formation mechanisms of viable but nonculturable bacteria through induction by light-based disinfection and their antibiotic resistance gene transfer risk: A review. *Crit. Rev. Environ. Sci. Technol.* **2022**, *52*, 3651−3688.
(41) Chen, S.; Li, X.; Wang, Y.; Zeng, J.; Ye, C.; Li, X.; Guo, L.; Zhang, S.; Yu, X. Induction of *Escherichia coli* into a VBNC state through chlorination/chloramination and differences in characteristics of the bacterium between states. *Water Res.* **2018**, *142*, 279−288.
(42) Yuan, Q.; Yu, P.; Cheng, Y.; Zuo, P.; Xu, Y.; Cui, Y.; Luo, Y.; Alvarez, P. J. J. Chlorination (but not UV disinfection) generates cell debris that increases extracellular antibiotic resistance gene transfer via proximal adsorption to recipients and upregulated transformation genes. *Environ. Sci. Technol.* **2022**, *56*, 17166−17176.
(43) Yin, H.; Cai, Y.; Li, G.; Wang, W.; Wong, P. K.; An, T. Persistence and environmental geochemistry transformation of antibiotic-resistance bacteria/genes in water at the interface of natural minerals with light irradiation. *Crit. Rev. Environ. Sci. Technol.* **2022**, *52*, 2270−2301.
(44) Imlay, J. A. The molecular mechanisms and physiological consequences of oxidative stress: lessons from a model bacterium. *Nat. Rev. Microbiol.* **2013**, *11*, 443−454.
(45) Chiang, S. M.; Schellhorn, H. E. Regulators of oxidative stress response genes in *Escherichia coli* and their functional conservation in bacteria. *Arch. Biochem. Biophys.* **2012**, *525*, 161−169.
(46) Taudte, N.; Grass, G. Point mutations change specificity and kinetics of metal uptake by ZupT from Escherichia coli. *BioMetals* **2010**, *23*, 643−656.
(47) Wang, H.; Yu, P.; Schwarz, C.; Zhang, B.; Huo, L.; Shi, B.; Alvarez, P. J. J. Phthalate esters released from plastics promote biofilm formation and chlorine resistance. *Environ. Sci. Technol.* **2022**, *56*, 1081−1090.
(48) Scott, S. R.; Hasty, J. Quorum sensing communication modules for microbial consortia. *ACS Synth. Biol.* **2016**, *5*, 969−977.
(49) Jenal, U.; Reinders, A.; Lori, C. Cyclic di-GMP: second messenger extraordinaire. *Nat. Rev. Microbiol.* **2017**, *15*, 271−284.
(50) Rumbaugh, K. P.; Sauer, K. Biofilm dispersion. *Nat. Rev. Microbiol.* **2020**, *18*, 571−586.

https://doi.org/10.1021/acsestwater.4c00603
ACS EST Water 2025, 5, 1546−1556

(51) Papenfort, K.; Bassler, B. L. Quorum sensing signal-response systems in Gram-negative bacteria. *Nat. Rev. Microbiol.* **2016**, *14*, 576−588.
(52) Thompson, J. A.; Oliveira, R. A.; Djukovic, A.; Ubeda, C.; Xavier, K. B. Manipulation of the quorum sensing signal AI-2 affects the antibiotic-treated gut microbiota. *Cell Rep.* **2015**, *10*, 1861−1871.
(53) Zhang, B.; Yu, P.; Wang, Z.; Alvarez, P. J. J. Hormetic promotion of biofilm growth by polyvalent bacteriophages at low concentrations. *Environ. Sci. Technol.* **2020**, *54*, 12358−12365.
(54) Wright, R. J.; Erni-Cassola, G.; Zadjelovic, V.; Latva, M.; Christie-Oleza, J. A. Marine Plastic Debris: A New Surface for Microbial Colonization. *Environ. Sci. Technol.* **2020**, *54* (19), 11657−11672.

https://doi.org/10.1021/acsestwater.4c00603
ACS EST Water 2025, 5, 1546−1556